

Noncooperative Virtual Queue Coordination via Uncertainty-Aware Correlated Equilibria

Jaehan Im, David Fridovich-Keil, Ufuk Topcu

Department of Aerospace Engineering

The University of Texas at Austin

Austin, Texas, USA

jaehan.im@utexas.edu, dfk@utexas.edu, utopcu@utexas.edu

Abstract—Collaborative virtual queueing has been proposed as a mechanism to mitigate airport surface congestion while preserving airline autonomy over aircraft-level pushback decisions. A central coordinator can regulate aggregate pushback capacity but cannot directly control which specific aircraft are released, limiting its ability to steer system-level performance. We propose a noncooperative coordination mechanism for collaborative virtual queueing based on the correlated equilibrium concept, which enables the coordinator to provide incentive-compatible recommendations on aircraft-level pushback decisions without overriding airline autonomy. To account for uncertainty in airlines' internal cost assessments, we introduce chance constraints into the correlated equilibrium formulation. This formulation provides explicit probabilistic guarantees on incentive compatibility, allowing the coordinator to adjust the confidence level with which airlines are expected to follow the recommended actions. We further propose a scalable algorithm for computing chance-constrained correlated equilibria by exploiting a reduced-rank structure. Numerical experiments demonstrate that the proposed method scales to realistic traffic levels up to 210 eligible pushbacks per hour, reduces accumulated delay by up to approximately 8.9% compared to current first-come-first-served schemes, and reveals a trade-off between confidence level, deviation robustness, and achievable cost efficiency.

Keywords—airport surface management; collaborative virtual queue; pushback control; noncooperative coordination; correlated equilibrium; decision making under uncertainty

I. INTRODUCTION

Airport surface congestion is increasingly managed through *collaborative virtual queue* (CVQ) systems [1]–[3]. CVQ improves airport surface operation efficiency by replacing physical queues on taxiways with a virtual abstraction thereby avoiding unnecessary engine-on delays. A key feature of CVQ is the division of authority, in which a central coordinator regulates aggregate gate pushback allowances per airline, whereas aircraft-level pushback decisions are made by individual airlines as illustrated in Figure 1.

The division of authority in CVQ however, introduces a practical coordination challenge. First, aircraft-level delay costs are airline-specific, time-varying, and private, making them difficult for a central authority to observe or verify. Second, system-level performance is sensitive to which aircraft

This work was supported by the National Aeronautics and Space Administration ULI Award under grants 80NSSC21M0071 and 80NSSC24M0070, and by the National Science Foundation CAREER award under grants 2336840 and 2211548.

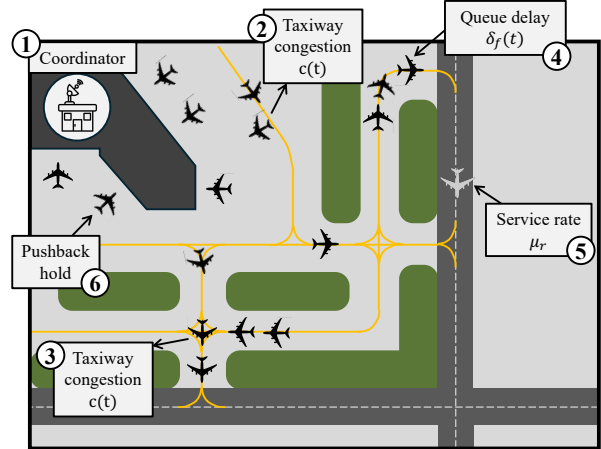


Figure 1. Illustration of the collaborative virtual queue coordination setting. A central coordinator regulates aggregate pushback capacity ① but does not control aircraft-level decisions directly. Released aircraft contribute to taxiway congestion $c(t)$ ②–③ and to runway queue delay $\delta_f(t)$ ④, while departures are governed by runway service rates μ_r ⑤. Airlines retain autonomy over pushback decisions ⑥, creating a noncooperative coordination problem.

airlines choose to push back and to the internal decision policies they employ for aircraft selection. Even under identical pushback allowances, uncoordinated airline-specific heuristics can lead to different congestion patterns and surface efficiency outcomes [1], [2]. As a result, existing CVQ approaches, which primarily focus on pushback capacity allocation while treating airlines' internal aircraft selection policies as a black box, provide the coordinator with limited ability to steer aircraft-level decisions toward system-optimal outcomes.

We address this limitation by developing a noncooperative coordination mechanism that preserves airline autonomy while enabling the coordinator to actively steer system-level outcomes. Rather than overriding airline decisions or imposing centralized control, we leverage the concept of *correlated equilibrium* to provide incentive-aligned recommendations on which aircraft to pushback, in addition to how many. By design, following the recommended action is rational for each airline given its cost structure, promoting voluntary compliance

Despite its theoretical appeal, correlated equilibrium relies

on exact knowledge of agents' cost functions, which is unrealistic in CVQ settings. To account for uncertainty in airlines' internal cost assessments, we propose an uncertainty-aware correlated equilibrium framework. Formally, this uncertainty awareness is captured through a *chance-constrained correlated equilibrium* (CC-CE), which ensures that the coordinator's guidance is incentive compatible with at least a user-specified probability.

We further develop a scalable algorithm to compute CC-CE by exploiting a *reduced-rank correlated equilibrium* structure [4]. By reconstructing a tractable subset of correlated equilibria from multiple pure Nash equilibria, the proposed approach significantly reduces the computational burden associated with direct correlated equilibrium computation. This enables practical deployment of CC-CE in large-scale virtual queue settings.

The contributions of this work are threefold. First, we reformulate the virtual queue coordination problem to enable aircraft-level influence via a noncooperative coordination mechanism. By leveraging correlated signaling, the proposed approach allows a CVQ coordinator to steer which specific aircraft are pushed back, while fully preserving airline autonomy. Second, we introduce a chance-constrained correlated equilibrium formulation that explicitly accounts for uncertainty in airlines' internal cost assessments. The proposed formulation provides a probabilistic guarantee on incentive compatibility, allowing the coordinator to quantify the confidence level with which airlines are expected to follow recommended actions under uncertain cost realizations. Third, we develop a scalable algorithm for computing CC-CE by exploiting a reduced-rank correlated equilibrium structure [4], enabling tractable computation in large-scale CVQ settings.

II. RELATED WORKS

A. Collaborative virtual queueing

Collaborative virtual queueing (CVQ) has been proposed as a mechanism to mitigate airport surface congestion by regulating gate departure pushbacks while preserving airline autonomy over aircraft-level decisions [1], [2], [5]. It aims to smooth surface traffic and reduce unnecessary taxiing and holding, reflecting the fact that congestion bottlenecks in busy airports typically arise near the runway rather than at the gate [6].

A substantial body of prior work on airport surface management formulates pushback, taxi, and runway sequencing as centralized optimization problems [7]–[9], including mixed-integer programs [10]–[13], neural network-based approaches [14], and route-optimization schemes [15]. These methods are effective when a single decision maker can enforce aircraft-level actions, but they abstract away airline autonomy and strategic behavior by assuming full centralized control.

Such centralized formulations are misaligned with the authority structure of CVQ. In CVQ operations, airlines retain control over which specific flights are pushed back within allocated slots as part of collaborative decision making [3]. Consequently, CVQ cannot directly influence airlines' internal flight-selection policies, and system-level performance may

still degrade due to airline-specific decision heuristics [1], [2].

In a similar spirit, several noncooperative and game-theoretic approaches have been explored in related air traffic and mobility contexts, although not directly in the virtual queueing setting [16]–[20]. These studies demonstrate how taxation [20], bilevel formulations [16], or auction mechanisms [17], [20] can guide stakeholder behavior without assuming centralized enforcement. However, they typically do not model the interactive decision-making among competing airlines [16] and often rely on strong assumptions such as truthful reporting [17], or fixed cost models without explicitly accounting for uncertainty in stakeholders' internal cost structures [4], [16]–[18], [20].

B. Correlated equilibria under uncertainty

The correlated equilibrium concept, introduced by Aumann as a generalization of the Nash equilibrium [21], has been widely studied as a mechanism for coordinating noncooperative agents, as it allows a coordinator to influence joint behavior while respecting individual's ability to make decisions that optimize their own objectives [4], [22], [23]. Existing work on correlated equilibria under uncertainty can be broadly grouped into several branches [24]–[29].

One line of research studies Bayes correlated equilibria, which model payoff uncertainty through states, types, and information structures and define rationality in terms of conditional expected utilities [24], [26]. In these formulations, uncertainty arises from players having incomplete information about payoff-relevant states or types; conditional on a given state, payoffs are deterministic. As a result, incentive compatibility is defined in expectation with respect to players' beliefs, rather than through explicit probabilistic guarantees on realized deviation gains [24], [26], [28], [29].

Other class of approaches models uncertainty directly in the agents' cost function through robust or distributionally robust formulations [25], [27], [28], [30], [31]. By enforcing worst-case guarantees over all admissible realizations or distributions of the payoff uncertainty within an ambiguity-set, these methods offer strong robustness but often lead to nonconvex optimization problems [30], [31]. As a result, they cannot fully exploit the linear and convex structure of the classical correlated equilibrium problem and may be overly conservative in applications where uncertainty arises from stochastic fluctuations around nominal costs.

Finally, bounded-rationality models such as quantal response equilibria and their correlated variants replace exact best responses with noisy, payoff-responsive choice rules [32], [33]. Equilibrium is defined as a fixed point of these stochastic response mappings. However, these models do not impose explicit probabilistic guarantees on profitable deviations; randomness is embedded in the response mechanism rather than regulated through deviation-based reliability constraints.

III. COLLABORATIVE VIRTUAL QUEUE PROBLEM

We formulate collaborative virtual queue (CVQ) coordination as a noncooperative game among airlines, with a ground controller acting as a coordinator. At each decision epoch,

a coordinator determines the aggregate pushback capacity, while airlines retain autonomy over aircraft-level pushback decisions. The coordinator does not enforce aircraft-level actions, but instead provides recommendations with the objective of minimizing system-level surface delay by influencing which aircraft are pushed back at each decision epoch.

A. Virtual queue coordination problem

Time is discretized into decision *epochs* indexed by $t \in \mathbb{Z}_{\geq 0}$. Let $R \in \mathbb{Z}_{>0}$ denote the number of departure runways at the airport and $\mathcal{F}(t)$ denote the set of aircraft eligible for pushback at epoch t . At each epoch t , the coordinator observes the surface state $s(t) := (q(t), \mathcal{F}(t)) \in \mathcal{S}$, where \mathcal{S} denotes the state space, and $q(t) \in \mathbb{Z}_{\geq 0}^R$ denotes the vector of runway queue lengths whose r -th entry $q_r(t)$ represents the number of aircraft physically waiting for departure at runway $r \in \{1, \dots, R\}$.

Let $\mathcal{I}(t)$ denote the set of airlines that have at least one eligible aircraft at epoch t . For each airline $i \in \mathcal{I}(t)$, let $\mathcal{F}_i(t) \subseteq \mathcal{F}(t)$ denote the subset of eligible aircraft operated by airline i .

1) *Airline actions*: For each active airline $i \in \mathcal{I}(t)$, let $\mathcal{X}_i(t)$ denote the set of feasible aircraft-level pushback actions available to airline i at epoch t . Airline i selects an action $x_i(t)$ defined as:

$$x_i(t) \in \mathcal{X}_i(t) := 2^{\mathcal{F}_i(t)}. \quad (1)$$

The resulting joint action is denoted by

$$x(t) := (x_i(t))_{i \in \mathcal{I}(t)} \in \mathcal{X}(t), \quad (2)$$

where $\mathcal{X}(t) := \prod_i \mathcal{X}_i(t)$. This action representation directly determines which aircraft enter the surface queues at epoch t .

2) *Eligible aircraft set dynamics*: Let $\mathcal{P}(t)$ denote the set of aircraft scheduled to depart at epoch t according to the published flight schedule. Each aircraft $f \in \mathcal{P}(t)$ is associated with a scheduled departure time τ_f , a designated departure runway $r(f) \in \{1, \dots, R\}$, and an aircraft class (e.g., small, medium, or heavy).

A set of aircraft that were in an eligible set but not pushed back in the previous epoch $t-1$ remain eligible in subsequent epoch t . Accordingly, the eligible aircraft set evolves as follows:

$$\mathcal{F}(t) = \mathcal{P}(t) \cup \{f \in \mathcal{F}(t-1) \mid f \notin \mathcal{D}(t-1)\}, \quad (3)$$

where $\mathcal{D}(t) := \bigcup_{i \in \mathcal{I}(t)} x_i(t)$ denotes the aircraft that are physically pushed back in epoch t .

3) *Runway queue dynamics*: Let runway service rate $\mu_r \in \mathbb{Z}_{\geq 0}$ denote the number of aircraft that departs from runway r per epoch, and let

$$a_r(t) := \sum_{f \in \mathcal{D}(t)} \mathbf{1}\{r(f) = r\}, \quad (4)$$

where $\mathbf{1}$ is an indicator function. (4) denote the number of aircraft pushed back to runway r at epoch t . The runway queue evolves according to

$$q_r(t+1) = \max\{0, q_r(t) + a_r(t) - \mu_r\}, \quad \forall r. \quad (5)$$

4) *Surface state evolution*: Combining (3) and (5), the surface state evolves according to

$$s(t+1) = g(s(t), x(t)), \quad (6)$$

where g captures both runway service dynamics and the evolution of the eligible aircraft set.

5) *Airline costs*: Airlines are modeled as noncooperative agents minimizing individual operational costs. At epoch t , airline i incurs a cost

$$J_i^t : \mathcal{X}(t) \times \mathcal{S} \rightarrow \mathbb{R}. \quad (7)$$

The cost $J_i^t(x(t); s(t))$ captures aircraft class-weighted delay and congestion effects induced by the joint pushback decisions and the resulting surface dynamics. For simplicity, we assume that airlines myopically optimize (7) at the current t and do not consider future costs.

6) *Coordinator objective*: The coordinator evaluates joint actions using a system-level objective

$$J_{\text{coord}}^t : \mathcal{X}(t) \times \mathcal{S} \rightarrow \mathbb{R}, \quad (8)$$

which aggregates aircraft-level delays over the epoch following the pushback decisions. The mechanism by which the coordinator induces an action introduced in Section IV.

B. Incorporating airline cost uncertainty

The coordinator does not observe airlines' true cost functions J_i^t . Instead, it maintains nominal cost models \bar{J}_i^t , which may differ from the airlines' realized operational costs.

We model this mismatch in terms of unilateral deviations. Specifically, for any fixed joint action profile (x_i, x_{-i}) and any unilateral alternative x'_i , the true deviation cost difference is assumed to satisfy

$$\begin{aligned} J_i(x_i, x_{-i}) - J_i(x'_i, x_{-i}) \\ = \bar{J}_i(x_i, x_{-i}) - \bar{J}_i(x'_i, x_{-i}) + \eta_i, \end{aligned} \quad (9)$$

where random variable $\eta_i \sim \nu_i$ represents airline-level uncertainty in deviation incentives and is drawn once per airline at each epoch. Importantly, η_i is common across all deviation comparisons for airline i within the same epoch.

In every epoch, each airline chooses an action $x_i(t)$ so as to minimize (7), while the coordinator's objective is to induce a joint action that minimizes (8). However, the coordinator cannot enforce aircraft-level actions or demand truthful disclosure of airline cost models. These issues motivate the proposed coordination mechanism, discussed below.

IV. COORDINATION VIA CORRELATED EQUILIBRIUM IN VIRTUAL QUEUE PROBLEM

The correlated equilibrium concept provides a coordination mechanism for noncooperative agents without requiring centralized enforcement. Rather than prescribing a deterministic joint action, a coordinator samples an action profile from a joint distribution and privately recommends that each agent follows the corresponding action. Following the recommendation is voluntary; nevertheless, rational agents find it optimal to comply when the distribution satisfies the correlated equilibrium conditions.

A. Correlated equilibrium

Formally, consider the game induced at a fixed surface state $s(t)$. Recall that $\mathcal{X} := \prod_{i \in \mathcal{I}(t)} \mathcal{X}_i(t)$ denotes the joint action space, and let $z \in \Delta(\mathcal{X})$ be a probability distribution over joint actions.

Definition 1 (Correlated Equilibrium). *A distribution $z \in \Delta(\mathcal{X})$ is a correlated equilibrium if the following holds:*

$$\mathbb{E}_{x_{-i} \sim z(\cdot|x_i)} [J_i(x_i, x_{-i}; s(t)) - J_i(x'_i, x_{-i}; s(t))] \leq 0, \quad (10)$$

for every airline i , every recommended action $x_i \in \mathcal{X}_i(t)$, and every unilateral deviation $x'_i \in \mathcal{X}_i(t)$.

The following lemma describes a basic geometric property of correlated equilibria.

Lemma 1 (Convexity of correlated equilibria). *The set of correlated equilibria is a convex subset of the probability simplex $\Delta(\mathcal{X})$.*

Proof. The constraints in (10) are linear in z , and $\Delta(\mathcal{X})$ is convex. Hence, the set of correlated equilibria is convex. \square

Under a correlated equilibrium z , the coordinator samples a joint action from z and privately recommends each component to the corresponding airline. Given z , each airline minimizes its expected cost conditional on the recommendation. By Definition 1, following the recommendation is incentive-compatible. Thus, the coordinator neither modifies airlines' objective functions nor enforces compliance; coordination arises naturally from incentive alignment. This makes correlated equilibrium well suited for collaborative virtual queues (CVQ), where airline autonomy must be preserved.

Example 1 (Coordination via correlation). *Consider a scenario where two drivers approach an intersection and choose either Go (G) or Stop (S). Their costs are given by*

	G	S
G	(5, 5)	(-1, 1)
S	(1, -1)	(1, 1)

(11)

where rows correspond to Driver 1 and columns to Driver 2. If both go, they incur a large penalty (5,5). If both stop, both incur a mild delay (1,1). If exactly one goes, the driver who goes benefits (-1) while the other incurs a mild delay (1). Consider a correlation device that selects (G, S) and (S, G) with probability $\frac{1}{2}$. If a driver is recommended to go, following the recommendation yields cost -1, whereas deviating leads to (S, S) with cost 1. If recommended to stop, following yields cost 1, whereas deviating leads to (G, G) with cost 5. Thus, conditioned on the received signal, deviation strictly increases cost. The correlation device therefore avoids collision or inefficient mutual stopping.

B. Chance-constrained correlated equilibrium

In practice, the coordinator does not have exact knowledge of airlines' cost functions. Deviation incentives are therefore uncertain and must be evaluated probabilistically. To account for this, we extend the correlated equilibrium concept.

For airline i , given an action profile (x_i, x_{-i}) and a deviation x'_i , define the deviation cost difference under the true model as

$$\Delta J_i(x_i, x'_i, x_{-i}) := J_i(x_i, x_{-i}) - J_i(x'_i, x_{-i}), \quad (12)$$

and under the nominal model as

$$\bar{\Delta} J_i(x_i, x'_i, x_{-i}) := \bar{J}_i(x_i, x_{-i}) - \bar{J}_i(x'_i, x_{-i}). \quad (13)$$

Recall that the realized deviation cost difference is subject to additive stochastic uncertainty,

$$\Delta J_i(x_i, x'_i, x_{-i}) = \bar{\Delta} J_i(x_i, x'_i, x_{-i}) + \eta_i, \quad (14)$$

where $\eta_i \sim \nu_i$ captures modeling error and operational variability in airline i 's cost. The disturbance η_i represents an airline-level common error and is assumed to be identical across all realizations of x_{-i} , rather than being resampled for each action profile. For numerical evaluation in Section V, we consider the special case $\nu_i = N(0, \sigma_i^2)$, where σ_i is measured in the same cost units as (14).

This leads to the following definition of a chance-constrained correlated equilibrium.

Definition 2 (Chance-constrained correlated equilibrium). *A distribution $z \in \Delta(\mathcal{X})$ is a chance-constrained correlated equilibrium (CC-CE) with confidence level $\alpha \in [0, 1]$ if,*

$$\mathbb{P}_{\nu_i} (\mathbb{E}_{x_{-i} \sim z(\cdot|x_i)} [\bar{\Delta} J_i(x_i, x'_i, x_{-i})] \leq 0) \geq \alpha, \quad (15)$$

for all airlines i , all recommended actions $x_i \in \mathcal{X}_i(t)$, and all deviations $x'_i \in \mathcal{X}_i(t) \setminus x_i$,

More generally, suppose that the deviation distribution ν_i admits a cumulative distribution function $\Phi_{\nu_i} : \mathbb{R} \rightarrow [0, 1]$. Then the chance constraint (15) can be expressed as:

$$\mathbb{E}_{x_{-i} \sim z(\cdot|x_i)} [\bar{\Delta} J_i(x_i, x'_i, x_{-i})] + \Phi_{\nu_i}^{-1}(\alpha) \leq 0, \quad (16)$$

where $\Phi_{\nu_i}^{-1}$ denotes the inverse cumulative distribution function of distribution ν_i .

An important property of CC-CE is that it preserves the convexity of the classical correlated equilibrium set as stated in lemma 1.

Theorem 1 (Convexity of CC-CE). *The feasible set of chance-constrained correlated equilibria is a convex polytope.*

Proof. Each chance constraint reduces to an affine inequality in the joint distribution z as shown in (16). Since $\Delta(\mathcal{X})$ is convex, the CC-CE feasible set is an intersection of finitely many affine half-spaces and is therefore a convex polytope. \square

The confidence level α explicitly quantifies the tradeoff between robustness and feasibility: larger α yields stronger incentive guarantees but shrinks the feasible set.

C. Scalable computation via reduced-rank correlated equilibria

Direct computation of correlated equilibrium is known for intractability to the number of the joint actions in the game. This problem holds in CC-CE computation and in virtual queue coordination problem as well since the joint action space grows exponentially with the number of airlines and aircraft. To address this challenge, we build on the reduced-rank correlated equilibrium (RRCE) framework [4].

RRCE approximates the correlated equilibrium polytope by the convex hull of a finite set of Nash equilibria, exploiting

the fact that Nash equilibria can be computed without enumerating all joint actions and are therefore computationally less demanding than solving for a correlated equilibrium directly. This idea relies on two classical results: every Nash equilibrium is a correlated equilibrium [34], and the set of correlated equilibria is convex (c.f., lemma 1)). We extend these ideas to computing the reduced-rank CC-CEs.

Definition 3 (Chance-constrained pure Nash equilibrium). *A pure strategy profile $x \in \mathcal{X}$ is a chance-constrained pure Nash equilibrium (CC-PNE) with confidence level α if,*

$$\mathbb{P}_{\nu_i}(\Delta J_i(x_i, x'_i, x_{-i}) \leq 0) \geq \alpha, \quad (17)$$

for every airline i and every unilateral deviation $x'_i \in \mathcal{X} \setminus x_i$.

The CC-PNE has a useful relationship to CC-CE as shown in the following lemma.

Lemma 2. *Every CC-PNE induces a CC-CE distribution.*

Proof. Let $x \in \mathcal{X}$ be a CC-PNE with confidence level α . By the definition of pure Nash equilibrium, the joint action distribution z concentrates all mass on x , i.e., $z(x) = 1$ and $z(\tilde{x}) = 0$ for all $\tilde{x} \neq x$. Thus, the following holds:

$$\begin{aligned} \mathbb{P}(\mathbb{E}_{\tilde{x}_{-i} \sim z(\cdot|x_i)} [\Delta J_i(x_i, x'_i, \tilde{x}_{-i})] \leq 0) \\ = \mathbb{P}(\Delta J_i(x_i, x'_i, x_{-i}) \leq 0). \end{aligned} \quad (18)$$

Since x is a CC-PNE, we can combine (17) with (18) yielding:

$$\mathbb{P}(\mathbb{E}_{\tilde{x}_{-i} \sim z(\cdot|x_i)} [\Delta J_i(x_i, x'_i, \tilde{x}_{-i})] \leq 0) \geq \alpha. \quad (19)$$

This completes the proof. \square

This observation extends naturally to convex combinations of CC-PNE.

Theorem 2. *The convex hull of CC-PNE distributions is a subset of the CC-CE feasible set.*

Proof. Every CC-PNE induces a CC-CE distribution by Lemma 2. Since the CC-CE feasible set is convex by Theorem 1, any convex combination of CC-PNE distributions also lies in the CC-CE set. \square

This result justifies extending the RRCE paradigm to the uncertainty-aware setting. By computing a finite collection of CC-PNE and constructing their convex hull, the coordinator can generate CC-CE distributions without solving the full CC-CE program. This approach significantly improves scalability in large instances [4].

D. Coordination via correlated equilibrium selection

We introduced the notion of correlated equilibrium and its chance-constrained extension to incorporate cost uncertainty, along with a reduced-rank construction for scalable computation. We now formalize the noncooperative coordination mechanism based on these equilibrium concepts.

At each decision epoch t , the coordinator does not enforce a deterministic joint action. Instead, it computes an optimal distribution $z \in \Delta(\mathcal{X}(t))$, samples a joint action $x \sim z$, and privately recommends to each airline its corresponding

component x_i . Compliance is voluntary as those recommendations are incentive-compatible to the airlines. Therefore, noncooperative coordination via this correlated equilibrium mechanism reduces to an equilibrium selection problem over the feasible CC-CE set.

1) Full CC-CE coordination problem: Recall that $J_{\text{coord}}^t(x; s(t))$ denotes the system-level objective evaluated at joint action $x \in \mathcal{X}(t)$. The expected system cost under distribution z is

$$\mathbb{E}_{x \sim z} [J_{\text{coord}}^t(x; s(t))] = \sum_{x \in \mathcal{X}(t)} z(x) J_{\text{coord}}^t(x; s(t)). \quad (20)$$

Then, the coordination problem based on CC-CE is formulated as:

$$\begin{aligned} \min_{z \in \Delta(\mathcal{X}(t))} \quad & \sum_{x \in \mathcal{X}(t)} z(x) J_{\text{coord}}^t(x; s(t)) \\ \text{s.t.} \quad & z \text{ satisfies (15).} \end{aligned} \quad (21)$$

Since the CC-CE constraints are affine in z and the simplex constraints are linear, (21) is a linear program. This formulation provides the optimal incentive-compatible coordination policy with $\alpha \in [0, 1]$ confidence.

2) Reduced-rank CC-CE coordination: To improve scalability, we restrict the feasible set to convex combinations of CC-PNE. Let $\{x^{(k)}\}_{k=1}^m$ denote a finite set of m CC-PNEs. Define the distribution

$$z(x) = \sum_{k=1}^m \lambda_k \mathbf{1}\{x = x^{(k)}\}, \quad \lambda \in \Delta_m, \quad (22)$$

where Δ_m is the m -dimensional simplex and $\mathbf{1}$ is an indicator function. Substituting (22) to (20) yields

$$\mathbb{E}_{x \sim z} [J_{\text{coord}}^t(x; s(t))] = \sum_{k=1}^m \lambda_k J_{\text{coord}}^t(x^{(k)}; s(t)). \quad (23)$$

Then, the reduced coordination problem becomes

$$\min_{\lambda \in \Delta_m} \quad \sum_{k=1}^m \lambda_k J_{\text{coord}}^t(x^{(k)}; s(t)). \quad (24)$$

By Theorem 2, every feasible solution of (24) induces a valid CC-CE distribution. This reduced formulation significantly lowers computational complexity, as it avoids enumerating the full joint action space and instead operates over a small set of CC-PNE.

In summary, noncooperative coordination in CVQ is achieved by solving an equilibrium selection problem: either the full CC-CE program (21) or its reduced-rank counterpart (24). The former provides optimal coordination under uncertainty, while the latter offers a scalable approximation suitable for large-scale airport operations.

V. NUMERICAL EXPERIMENT

A. Scenario description

We consider a collaborative virtual queue (CVQ) surface-operations scenario with each epoch corresponding to four minutes of real time. At each epoch, the coordinator observes the current runway queue lengths $q(t)$ and the set of

eligible aircraft $\mathcal{F}(t)$. Each aircraft $f \in \mathcal{F}(t)$ is associated with a designated runway $r(f)$ and an aircraft class (i.e., small/medium/heavy). Airlines select subsets of their eligible aircraft for pushback, inducing runway inflows $a_r(t)$. The runway queues evolve according to the dynamics introduced in Section III, with service rates μ_r aircraft per epoch. Airlines act according to their realized cost (14); in particular, deviation incentives are subject to additive Gaussian perturbations $\nu_i \sim \mathcal{N}(0, \sigma_i^2)$ that are unobserved by the coordinator. The overall CVQ coordination loop is illustrated in Figure 1.

1) *Costs and objectives*: We evaluate costs over the eligible flight set $\mathcal{F}(t)$ under the realized joint pushback decision $x(t)$. Let τ_f denote the scheduled departure time of flight f in minutes. Since each epoch represents four minutes, the accumulated lateness (in minutes) at epoch t is defined as

$$\ell_f(t) := \max\{0, 4t - \tau_f\}, \quad (25)$$

which captures realized schedule delay. We define the one-epoch waiting penalty

$$w_f(t) := \begin{cases} 0, & f \in \mathcal{D}(t), \\ 4, & f \notin \mathcal{D}(t), \end{cases} \quad (26)$$

where $\mathcal{D}(t)$ is the set of pushed flights; thus, a flight that is not released incurs an additional four-minute delay.

Let $\tilde{q}_r(t+1, x(t))$ denote the predicted next-epoch queue length at runway r induced by $x(t)$: $\tilde{q}_r(t+1, x(t)) = q_r(t) + a_r(t)$, where $a_r(t)$ is the number of flights in $x(t)$ assigned to runway r as defined in (4). The runway queue-induced delay for flight f is

$$\delta_f(t) = \frac{\tilde{q}_{r(f)}(t+1, x(t))}{\mu_{r(f)}} \cdot 4, \quad (27)$$

which approximates the expected waiting time (in minutes) required for proceeding aircraft in the departure queue to be served. We also include a taxiway congestion penalty

$$c(t) = (\max\{0, |\mathcal{D}(t)| - 4\})^2, \quad (28)$$

which reflects that the taxiway can accommodate up to four simultaneously released aircraft without congestion effects; additional releases beyond this threshold incur a quadratic penalty. The per-flight delay is

$$d_f(t) = \begin{cases} (\ell_f(t) + w_f(t))^2 + \delta_f(t) + c(t), & \ell_f(t) + w_f(t) > 10, \\ \ell_f(t) + w_f(t) + \delta_f(t) + c(t), & \text{otherwise.} \end{cases} \quad (29)$$

When the accumulated pushback delay $\ell_f(t) + w_f(t)$ exceeds 10 minutes, the airline incurs a quadratic penalty, reflecting increased airline/passenger dissatisfaction. This delay model reflects a trade-off between congestion from schedule delay from excessive pushbacks, and is consistent with commonly used delay models in departure-management studies [35].

Airline i minimizes the class-weighted delay

$$J_i^t(x(t); s(t)) = \sum_{f \in \mathcal{F}_i(t)} \omega_{c(f)} d_f(t), \quad (30)$$

where $\omega_{c(f)} \in \mathbb{R}_{\geq 0}$ is a weight determined by the aircraft class of flight f . In the experiments, we use

$[\omega_{\text{heavy}}, \omega_{\text{medium}}, \omega_{\text{small}}] = [1.2, 1.0, 0.75]$. The coordinator evaluates the unweighted total delay

$$J_{\text{coord}}^t(x(t); s(t)) = \sum_{f \in \mathcal{F}(t)} d_f(t). \quad (31)$$

Both airlines and the coordinator seek to reduce delay, but airlines apply class-dependent weights whereas the coordinator evaluates unweighted total delay. This reflects a standard distinction between airline objectives (e.g., fleet-dependent valuations) and an airport/coordinator objective that prioritizes aggregate throughput and surface delay [1], [2].

B. Evaluation metrics

We evaluate solver performance using three metrics:

a) *Delay cost*: We report the realized delay cost computed according to the cost model defined in (31). This metric captures both schedule delay and congestion-induced delay.

b) *Computation time*: We measure wall-clock computation time required to compute the equilibrium at each epoch.

c) *Deviation rate*: We report the deviation rate, defined as the fraction of trials in which at least one airline deviates from the recommended action.

C. Baseline algorithms

We compare five coordination mechanisms:

a) *CENT*: A fully centralized benchmark assuming complete control authority over all aircraft decisions. This provides an idealized lower bound on achievable cost.

b) *FCFS*: A decentralized first-come-first-served mechanism reflecting current operational practice [1], [2]. The coordinator solves the same aggregate capacity optimization problem as in *CENT*, but does not select specific aircraft. Each airline then independently selects the aircraft with the earliest scheduled departure.

c) *Full-CCCE*: A full correlated equilibrium solver that explicitly accounts for cost uncertainty using chance-constrained correlated equilibrium (CC-CE) formulation (21).

d) *RR-Nominal*: A reduced-rank correlated equilibrium (RRCE)-based solver that solves (24) under nominal costs, without accounting for cost uncertainty.

e) *RR-CCCE*: A RRCE-based solver that incorporates cost uncertainty into the equilibrium constraints.

Table I summarizes the key differences among the compared coordination mechanisms.

TABLE I. Comparison of coordination mechanisms

Method	CE formulation	Uncertainty-aware
CENT	–	–
FCFS	–	–
Full-CCCE	Full formulation (21)	Yes
RR-Nominal	Reduced formulation (24)	No
RR-CCCE	Reduced formulation (24)	Yes

Remark 1. For the RRCE-based methods, we compute the set of pure Nash equilibria by enumerating all joint actions and checking the equilibrium condition. While exhaustive enumeration is utilized, the considered single-epoch instances remain of moderate size, while reflecting realistic busy-airport conditions [36], making this approach computationally tractable.

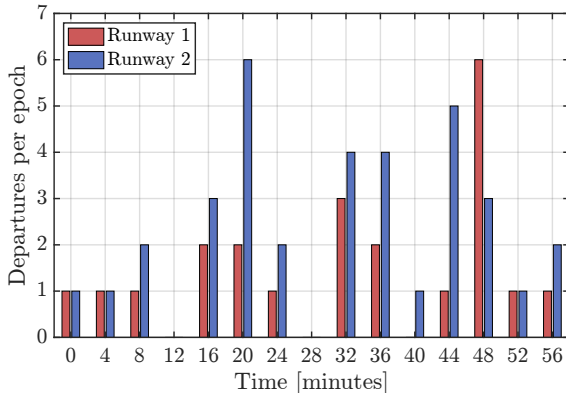


Figure 2. Departure rates per runway for each 4-minute epoch across a 60-minute horizon. Red and blue bars correspond to Runway 1 and Runway 2, respectively. The schedule is synthetically generated with an average departure rate of 1.05 flights per minute.

D. Experimental plan

We evaluate the proposed coordination mechanism at two levels. First, we conduct a single-epoch Monte Carlo experiment. This setting enables a controlled comparison of equilibrium computation and resulting costs across solvers. Second, we perform a 16-epoch (one-hour simulation time) experiment in which the single-epoch mechanism is applied sequentially. This experiment assesses cumulative delay behavior and demonstrates operational applicability.

1) *Experiment 1 (Single-epoch simulation):* In the single-epoch experiment, each trial randomly generates a busy-airport epoch instance. We fix the number of runways ($R = 2$), service rates ($[\mu_1, \mu_2] = [2, 2]$), and initial queue lengths $q(0) = [3, 4]$. The experimental variables are: (i) the eligible aircraft count $|\mathcal{F}(t)|$, (ii) the confidence level α , and (iii) the deviation-noise level σ introduced in Section IV-B. We evaluate $|\mathcal{F}(t)| \in \{6, 7, \dots, 14\}$, $\alpha \in [0.30, 0.99]$, and $\sigma \in [0, 45]$ (recall that σ is measured in the same cost units as (14)). For each eligible flight, scheduled lateness is independently drawn as $L_f \sim \mathcal{N}(0, 10^2)$ and truncated via $L_f \leftarrow \max\{0, L_f\}$, so that negative realizations correspond to on-time departures.

The aircraft count $|\mathcal{F}(t)| = 14$ per epoch corresponds to approximately 210 eligible pushbacks per hour. For reference, Hartsfield-Jackson Atlanta International Airport—one of the busiest airports worldwide—processes roughly 96 departures per hour [36]. Thus, the tested range spans realistic and congested regimes.

2) *Experiment 2 (Multi-epoch rolling simulation):* The multi-epoch experiment evaluates rolling deployment over a one-hour horizon (16 epochs). The system starts from empty queues, $q(0) = [0, 0]$. A single departure schedule is generated according to the following specification and kept fixed across experiments. Aircraft arrivals follow a Poisson process with an arrival rate of 1.05 aircraft per minute, slightly exceeding the nominal system capacity of 1 aircraft per minute (two runways, each serving 2 aircraft per 4-minute epoch). Aircraft classes are generated with probabilities 0.4 (small), 0.3 (medium), and 0.3 (heavy), and each flight

is randomly assigned to one of five airlines. A departure schedule used in the simulation is shown in Figure 2. Across experiments, only the cost noise level σ is varied, while the underlying traffic instance remains unchanged.¹

Remark 2 (Implementation details). *The experiments were implemented in Julia v1.11.3. We used the packages ParametricMCP [37] and PATHSolver [38] with default convergence tolerances to compute correlated equilibria. All simulations were executed on a Linux computer equipped with an Intel Core i7-12700 CPU and 16 GB RAM. Each Monte Carlo experiment consisted of 100 independent trials with fixed random seeds for reproducibility.*

E. Single-epoch experiment result

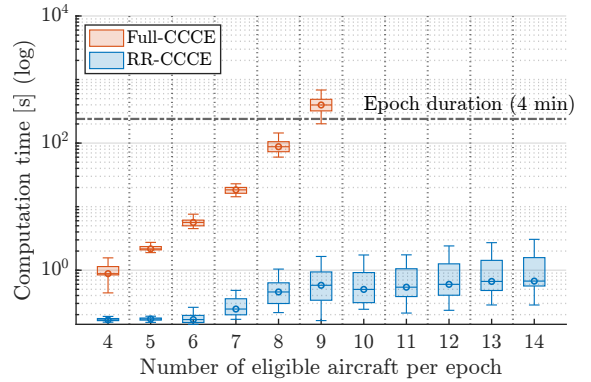


Figure 3. Scalability comparison between Full-CCCE and RR-CCCE. Wall-clock computation time (log scale) is shown as a function of the number of eligible aircraft per epoch. The horizontal dotted line indicates the epoch duration (4 minutes), representing the real-time constraint for online deployment. Median marked by \circ .

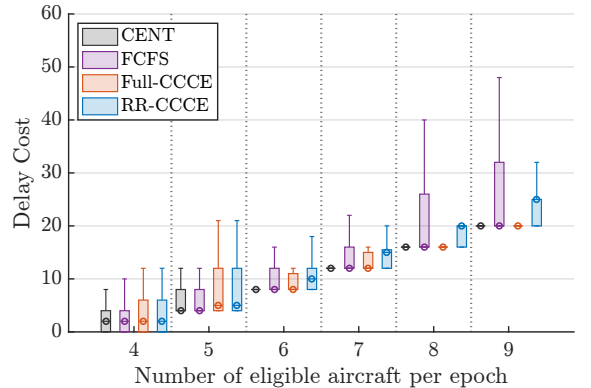
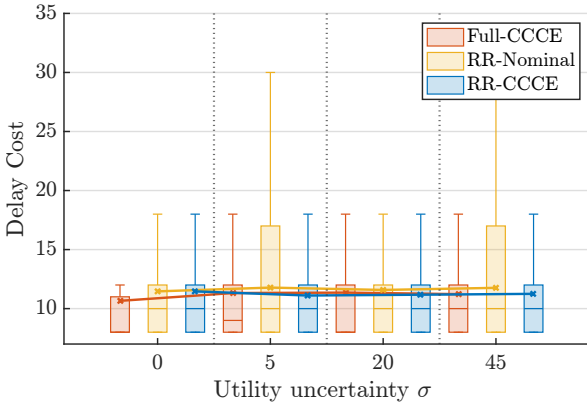


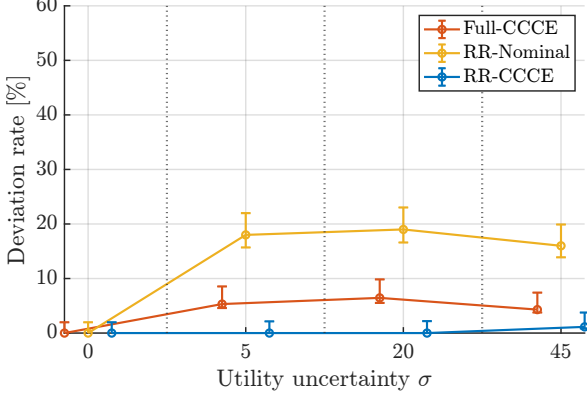
Figure 4. Comparison of realized delay cost across coordination mechanisms. CENT serves as an idealized performance benchmark. Full-CCCE and RR-CCCE outperform FCFS as traffic increases. RR-CCCE exhibits a performance gap relative to Full-CCCE due to equilibrium-set approximation. Median marked by \circ .

1) *Scalability benefit of CC-CE approximation:* To assess the scalability of RR-CCCE, we compare it with Full-CCCE. Figure 3 shows wall-clock computation time

¹If a correlated equilibrium-based solver fails to compute a feasible solution (e.g., no equilibrium found or computation time exceeds the epoch duration), the mechanism defaults to FCFS for that epoch.



(a)



(b)

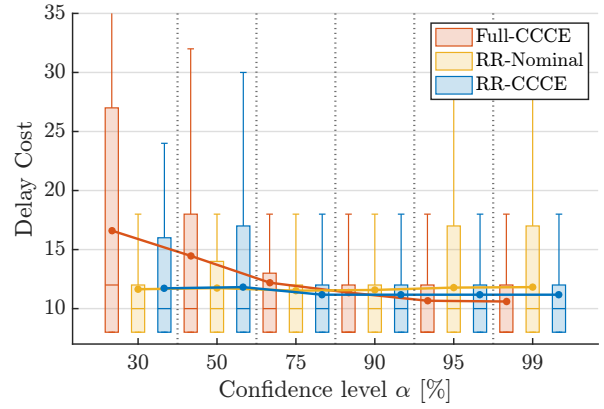
Figure 5. Performance under cost uncertainty ($\alpha = 90\%$, six airlines). (a) Delay cost distribution as a function of cost noise level σ . (b) Deviation rate versus σ . Horizontal lines within boxplots indicate mean values.

as the number of eligible aircraft increases from 6 to 14. For Full-CCCE, computation time grows rapidly due to the exponential expansion of the joint-action space, which scales on the order of $2^{|\mathcal{F}(t)|}$. RR-CCCE remains well below the 4-minute epoch duration, while Full-CCCE exceeds this real-time threshold at 9 aircraft per epoch.

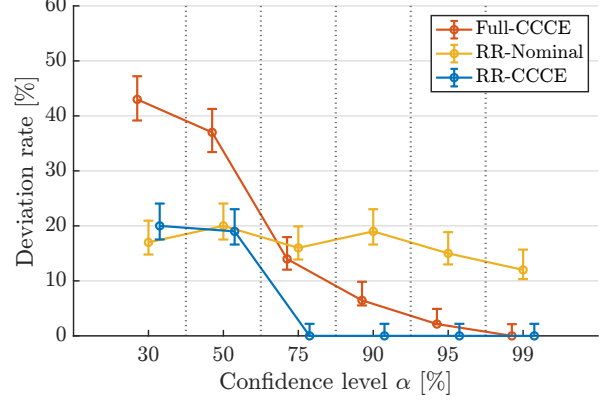
2) *Delay cost*: We compare the realized delay cost of the solution outcomes across solvers under $\sigma = 0$. Figure 4 shows the cost as the number of eligible aircraft increases.

CENT serves as an idealized benchmark assuming full control authority and is included for reference. At low traffic levels, medians are similar, though Full-CCCE and RR-CCCE show higher variance. As traffic increases, the costs for FCFS rises sharply whereas uncertainty-aware methods yield lower costs. In the high-volume regime (8–9 aircraft per epoch), Full-CCCE achieves performance comparable to CENT. RR-CCCE exhibits a modest performance degradation relative to Full-CCCE, due to the reduced-rank approximation of the equilibrium set.

3) *Performance under uncertainty*: We evaluate uncertainty robustness by comparing Full-CCCE, RR-Nominal, and RR-CCCE. The number of airlines is fixed to six. When varying the cost noise level σ , the confidence level is fixed at $\alpha = 90\%$. When varying α , the noise level is fixed at $\sigma = 20$.



(a)



(b)

Figure 6. Performance under varying confidence levels ($\sigma = 20$, six airlines). (a) Delay cost distribution as a function of confidence level α . (b) Deviation rate versus α . Horizontal lines within boxplots indicate mean values.

a) *Effect of cost uncertainty (σ)*: As shown in Figure 5, the mean delay costs remain comparable across all methods over the range of uncertainty levels. While most algorithms exhibit relatively stable cost distributions, RR-Nominal shows a mild increase in variance in the high-uncertainty regime. Overall, the delay performance remains largely consistent across methods as σ increases.

Regarding deviation frequency, uncertainty-aware methods demonstrate improved robustness. Notably, under $\alpha = 90\%$, Full-CCCE exhibits deviation rates roughly aligned with the confidence level, whereas RR-CCCE maintains near-zero deviation frequency across all tested σ values.

b) *Effect of confidence level (α)*: As the confidence level α increases, deviation rates for Full-CCCE start from relatively high levels and gradually decline. RR-CCCE maintains the lowest deviation rate overall and approaches zero deviation for $\alpha \geq 75\%$. In contrast, RR-Nominal remains with deviation rates consistently in the 10–20% range across α . These trends are illustrated in Figure 6.

In terms of delay cost, Full-CCCE shows a decreasing trend as α increases. The mean costs for the others remain relatively stable across α , with the smallest variance and mean value observed around $\alpha \in [0.90, 0.99]$.

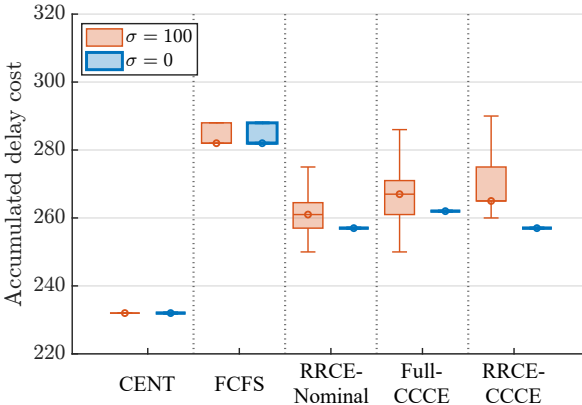


Figure 7. Accumulated delay cost over a 16-epochs rolling simulation. Two uncertainty settings are compared: $\sigma = 0$ and $\sigma = 100$. Each boxplot summarizes repeated runs with identical traffic realization and varying cost noise. Median marked by \circ .

F. Multi-epoch experiment result

We evaluate the rolling deployment of each coordination mechanism over a one-hour horizon (16 epochs). The accumulated cost over the horizon reflects repeated application of the single-epoch policy rather than a long-horizon optimal solution. This experiment evaluates cumulative effects and operational scalability.

Across both high- and low- σ scenarios, correlated equilibrium-based methods achieve approximately 6.0–7.4% reduction in accumulated delay compared to FCFS as shown in Figure 7. When $\sigma = 0$, this improvement increases to approximately 7.1–8.9%. Under large uncertainty ($\sigma = 100$), RR-Nominal sometimes achieves lower accumulated cost than uncertainty-aware variants. This reflects a trade-off between diverse profile selection and robustness: nominal coordination can exploit high-performing equilibria but tolerates higher deviation risk.

VI. DISCUSSION

A. Coordination benefit over first-come-first-served (FCFS)

Across both low- and high-uncertainty settings, correlated equilibrium-based coordination consistently reduces accumulated delay compared to FCFS, which reflects current CVQ first-come-first-served operations. This confirms that providing incentive-compatible aircraft-level recommendations improves system-level performance without requiring centralized control authority. The improvement is more pronounced in low-uncertainty environments, where deviation is limited and recommended profiles are more reliably implemented.

B. Confidence level, deviation, and feasible set

A key observation concerns the interaction between confidence level α , deviation rate, and cost performance under uncertainty. As expected, increasing α reduces the empirical deviation rate. This reflects the widening of incentive margins in the chance-constrained equilibrium conditions. At the same time, increasing α contracts the feasible CC-CE region, and in some instances reduces the number of available equilibrium profiles or increases solver failure rates. A similar contraction

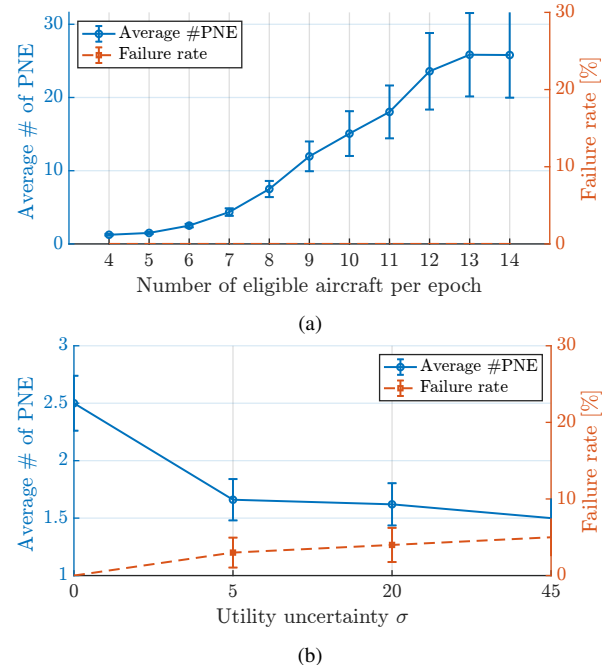


Figure 8. Equilibrium-space characteristics. (a) Average number of chance-constrained pure Nash equilibria (CC-PNE) and solver failure rate as the number of eligible aircraft increases ($\alpha = 90\%$, $\sigma = 20$). (b) Average number of CC-PNE and failure rate as cost uncertainty σ increases ($|\mathcal{F}(t)| = 8$, $\alpha = 90\%$). Increasing problem size expands the equilibrium set, whereas higher uncertainty reduces discoverable equilibria and increases failure probability.

effect is observed when cost uncertainty σ increases as illustrated in Figure 8.

While the relationship between α and both deviation rate and the size of the feasible equilibrium region is structurally clear, its effect on realized cost is more nuanced. Reducing deviation increases the likelihood that the recommended profile is implemented, but shrinking the feasible equilibrium region may eliminate high-performing profiles. This trade-off is visible in the experiments.

In the single-epoch setting, RR-CCCE and Full-CCCE improve median cost as α increases from 30% to 75% and the deviation rate drops (Figure 6). However, the performance of Full-CCCE slightly exceeds that of RR-CCCE in the $\alpha \in [0.95, 0.99]$ regime, and even Full-CCCE emits a nonzero deviation rate. A similar pattern is observed in the multi-epoch setting, where RR-Nominal sometimes achieves lower accumulated cost under high noise, at the expense of a higher deviation frequency. This does not contradict the robustness objective; rather, it highlights the risk–performance trade-off inherent in chance-constrained coordination.

C. Algorithmic trade-offs

Differences between full and reduced formulations further highlight this structural trade-off. Figure 6 shows that RR-CCCE exhibits substantially lower deviation rates than Full-CCCE at identical confidence levels. This can be interpreted as a consequence of the reduced space of equilibria: the reduced-rank approximation limits the available profiles but implicitly increases robustness. Overall, the results suggest

the existence of a confidence-level “sweet spot”, balancing profile diversity and implementation reliability.

VII. CONCLUSION

We proposed a chance-constrained correlated equilibrium framework for collaborative virtual queue coordination under airline cost uncertainty. The formulation provides probabilistic incentive guarantees and allows explicit adjustment of confidence levels. A reduced-rank approach was developed to enable scalable computation.

Numerical experiments demonstrate scalability up to traffic levels corresponding to 210 aircraft eligible for pushback per hour—consistent with operations at the world’s busiest airports—and show up to an 8–9% reduction in accumulated delay compared to the current first-come-first-served mechanism. The results further reveal a trade-off among confidence level, deviation frequency, and cost efficiency.

Future work includes characterizing conditions under which pure Nash equilibria cease to exist under high uncertainty and systematically identifying optimal confidence-level operating points that balance robustness and performance.

REFERENCES

- [1] D. Bhadra, D. A. Knorr, and B. Levy, “Benefits of virtual queuing at congested airports using asde-x: A case study of jfk airport,” *Air Traffic Control Q.*, vol. 20, no. 3, pp. 225–251, 2012.
- [2] P. Burgain, E. Feron, and J.-P. Clarke, “Collaborative virtual queue: Benefit analysis of a collaborative decision making concept applied to congested airport departure operations,” *Air Traffic Control Q.*, vol. 17, no. 2, pp. 195–222, 2009.
- [3] L. A. Wojcik, S. L. Mondoloni, S. J. Agbolosu-Amison, and P. Wang, “Flexibility metrics and their application to departure queue management,” in *Tenth USA/Europe Air Traffic Manage. Res. Develop. Semin. (ATM2013)*, Chicago, 2013.
- [4] J. Im, Y. Yu, D. Fridovich-Keil, and U. Topcu, “Coordination in noncooperative multiplayer matrix games via reduced rank correlated equilibria,” *IEEE Control Syst. Lett.*, vol. 8, pp. 1637–1642, 2024.
- [5] R. De Lange, I. Samoilovich, and B. Van Der Rhee, “Virtual queuing at airport security lanes,” *Eur. J. Oper. Res.*, vol. 225, no. 1, pp. 153–165, 2013.
- [6] J. Lai, L. Che, and R. Kashef, “Bottleneck analysis in jfk using discrete event simulation: an airport queuing model,” in *2021 IEEE Int. Smart Cities Conf. (ISC2)*. IEEE, 2021, pp. 1–7.
- [7] Y. Eun, D. Jeon, H. Lee, Y. C. Jung, Z. Zhu, M. Jeong, H. Kim, E. Oh, and S. Hong, “Optimization of airport surface traffic: A case-study of incheon international airport,” in *17th AIAA Aviation Technology, Integration, and Operations Conf.*, 2017, p. 4258.
- [8] Y. Eun, D. Jeon, H. Kim, Y. Jung, H. Lee, Z. Zhu, and V. Hosagrahara, “A tactical scheduler for surface metering under minimum departure interval restrictions,” in *2019 IEEE/AIAA 38th Digit. Avionics Syst. Conf. (DASC)*. IEEE, 2019, pp. 1–10.
- [9] R. Deau, J.-B. Gotteland, and N. Durand, “Airport surface management and runways scheduling,” in *ATM 2009, 8th USA/Europe Air Traffic Manage. Res. Develop. Semin.*, 2009, pp. pp–xxxx.
- [10] H. Balakrishnan, “Control and optimization algorithms for air transportation systems,” *Annu. Rev. Control*, vol. 41, pp. 39–46, 2016.
- [11] I. Simaiakis, “Analysis, modeling and control of the airport departure process,” Ph.D. dissertation, Massachusetts Inst. Technol., 2013.
- [12] K. Gopalakrishnan and H. Balakrishnan, “Privacy and stability in airport ground delay programs,” in *2017 IEEE 56th Annu. Conf. Decis. Control (CDC)*. IEEE, 2017, pp. 1199–1205.
- [13] H. Balakrishnan and B. Chandran, “Efficient and equitable departure scheduling in real-time: new approaches to old problems,” in *7th USA-Europe Air Traffic Manage. Res. Develop. Semin.*, 2007, pp. 02–05.
- [14] L. P. McKenna, K. Chour, M. Memarzadeh, K. Kalyanam, and R. Sharma, “A neural-queuing approach to modeling airport surface traffic at charlotte-douglas international airport,” in *AIAA Aviation Forum and ASCEND 2025*, 2025, p. 3444.
- [15] S. Imai, S. Patterson, and C. A. Varela, “Elastic virtual machine scheduling for continuous air traffic optimization,” in *2016 16th IEEE/ACM Int. Symp. Cluster, Cloud Grid Comput. (CCGrid)*. IEEE, 2016, pp. 183–186.
- [16] H. Wu, L. A. Weitz, J. M. Henderson, and M. Z. Li, “Optimization-guided exploration of advanced air mobility congestion management strategies with stochastic demands,” *arXiv preprint arXiv:2509.18505*, 2025.
- [17] M. Raffarin, “Auction mechanism to allocate air traffic control slots,” in *The Conf. Proc. 2003 Air Transp. Res. Soc. (ATRS) World Conf.*, Vol. 2, 2003.
- [18] J. Im, D. Delahaye, D. Fridovich-Keil, and U. Topcu, “Game-theoretic decentralized coordination for airspace sector overload mitigation,” *arXiv preprint arXiv:2511.13770*, 2025.
- [19] J. Im and J. Ahn, “Decentralized free-flow traffic management based on nash equilibrium,” *J. Aerosp. Inf. Syst.*, vol. 20, no. 4, pp. 195–203, 2023.
- [20] J. Im, J.-P. Clarke, U. Topcu, and D. Fridovich-Keil, “Iterative negotiation and oversight: A case study in decentralized air traffic management,” *arXiv preprint arXiv:2511.17625*, 2025.
- [21] R. J. Aumann, “Correlated equilibrium as an expression of bayesian rationality,” *Econometrica*, pp. 1–18, 1987.
- [22] Y. Ning and L. Du, “Robust and resilient equilibrium routing mechanism for traffic congestion mitigation built upon correlated equilibrium and distributed optimization,” *Transp. Res. Part B: Methodol.*, vol. 168, pp. 170–205, 2023.
- [23] J. Duffy, E. K. Lai, and W. Lim, “Coordination via correlation: An experimental study,” *Econ. Theory*, vol. 64, no. 2, pp. 265–304, 2017.
- [24] K. D. Cotter, “Correlated equilibria with payoff uncertainty,” Discussion Paper, Tech. Rep., 1989.
- [25] D. Bergemann and S. Morris, “Robust predictions in games with incomplete information,” *Econometrica*, vol. 81, no. 4, pp. 1251–1308, 2013.
- [26] K. D. Cotter, “Correlated equilibria with payoff uncertainty,” Discussion Paper, Tech. Rep., 1989.
- [27] A. Hori and N. Yamashita, “Two-stage distributionally robust noncooperative games: Existence of nash equilibria and its application to cournot–nash competition,” *J. Ind. Manage. Optim.*, 2022.
- [28] Z. Chen, S. Ma, and Y. Zhou, “Finding correlated equilibrium of constrained markov game: A primal-dual approach,” *Adv. Neural Inf. Process. Syst.*, vol. 35, pp. 25 560–25 572, 2022.
- [29] R. Misra, R. Wiśniewski, C. S. Kallesøe, and M. L. Bujorianu, “Robust correlated equilibrium: Definition and computation,” *Automatica*, vol. 184, p. 112719, 2026.
- [30] N. Loizou, “Distributionally robust game theory,” *arXiv preprint arXiv:1512.03253*, 2015.
- [31] Y. Liu, H. Xu, S.-J. S. Yang, and J. Zhang, “Distributionally robust equilibrium for continuous games: Nash and stackelberg models,” *Eur. J. Oper. Res.*, vol. 265, no. 2, pp. 631–643, 2018.
- [32] T. Ui, “Correlated quantal responses and equilibrium selection,” *Games Econ. Behav.*, vol. 57, no. 2, pp. 361–369, 2006.
- [33] J. Černý, B. An, and A. N. Zhang, “Quantal correlated equilibrium in normal form games,” in *Proc. 23rd ACM Conf. Econ. Comput.*, 2022, pp. 210–239.
- [34] R. Nau, S. G. Canovas, and P. Hansen, “On the geometry of nash equilibria and correlated equilibria,” *Int. J. Game Theory*, vol. 32, no. 4, pp. 443–453, 2004.
- [35] L. A. Wojcik, S. L. Mondoloni, S. J. Agbolosu-Amison, P. Wang, and V. McLean, “Flexibility metrics and their application to departure queue management,” in *10th USA/Europe air traffic management research and development seminar*, 2013.
- [36] G. Yablonsky, R. Steckel, D. Constales, J. Farnan, D. Lercel, and M. Patankar, “Flight delay performance at hartsfield-jackson atlanta international airport,” *J. Airline Airport Manage.*, vol. 4, no. 1, pp. 78–95, 2014.
- [37] L. Peters, “ParametricMCPs.jl,” 2022. [Online]. Available: <https://github.com/lassepe/ParametricMCPs.jl>
- [38] S. P. Dirkse and M. C. Ferris, “The path solver: a nonmonotone stabilization scheme for mixed complementarity problems,” *Optim. Methods Softw.*, vol. 5, no. 2, pp. 123–156, 1995.